Qu et al. Stem Cell Research & Therapy (2024) 15:496
https://doi.org/10.1186/s13287-024-04111-6

Stem Cell Research & Therapy

RESEARCH Open Access

Exosomes derived from hypoxic mesenchymal stem cells restore ovarian function by enhancing angiogenesis

Qingxi Qu[1], Linghong Liu[2,3*], Limei Wang[1], Yuqian Cui[1], Chunxiao Liu[4], Xuanxuan Jing[5] and Xiaoxuan Xu[1]

Abstract

Background hucMSC-exosomes can be engineered to strengthen their therapeutic potential, and the present study aimed to explore whether hypoxic preconditioning can enhance the angiogenic potential of hucMSC-exosomes in an experimental model of POF.

Methods Primary hucMSCs and ROMECs were isolated from fresh tissue samples and assessed through a series of experiments. Exosomes were isolated from hucMSCs under normoxic or hypoxic conditions (norm-Exos and hypo-Exos, respectively) and then characterized using classic experimental methods. Based on a series of angiogenesis-related assays, we found that hypo-Exos significantly promoted ROMEC proliferation, migration, and tube formation and increased angiogenesis-promoting molecules in vitro. Histology, immunohistochemistry, and immunofluorescence experiments in a rat model of POF demonstrated that hypoxia pretreatment strengthens the therapeutic angiogenic effect of hucMSC-exosomes in vivo. Subsequently, high-throughput miRNA sequencing, qRT-PCR analysis, and western blotting were employed to identify the potential molecular mechanism.

Results We found that hypo-Exos enhance endothelial function and angiogenesis via the transfer of miR-205-5p in vitro and in vivo. Finally, based on the results of bioinformatics analysis, dual luciferase reporter assays, and gain- and loss-of-function studies, we found evidence indicating that exosomal miR-205-5p enhances angiogenesis by targeting the PTEN/PI3K/AKT/mTOR signalling pathway. These results indicated for the first time that exosomes derived from hypoxia-conditioned hucMSCs strongly enhance angiogenesis via the transfer of miR-205-5p by targeting the PTEN/PI3K/AKT/mTOR signalling pathway.

Conclusions Our findings provide a theoretical basis and demonstrate the potential application of a novel cell-free approach with stem cell-derived products in the treatment of POF.

Keywords Premature ovarian failure, Hypoxic preconditioning, Exosomes, Mesenchymal stem cells, Angiogenesis, miR-205-5p, PTEN

*Correspondence:
Linghong Liu
llh19911028@126.com
[1]Department of Obstetrics and Gynecology, Qilu Hospital of Shandong University, Jinan 250012, P.R. China
[2]Research Center of Stem Cell and Regenerative Medicine, Shandong University, Jinan 250012, P.R. China
[3]Laboratory of Cryomedicine, Qilu Hospital of Shandong University, Jinan 250012, P.R. China
[4]Department of Cardiovascular Surgery, Qilu Hospital of Shandong University, Jinan 250012, P.R. China
[5]Department of Ultrasound, Qilu Hospital of Shandong University, Jinan 250012, P.R. China

Introduction

Premature ovarian failure (POF) is a common endocrine disease clinically defined as loss of ovarian function in women less than 40 years of age. POF is characterized by abnormal menstruation, abnormally increased follicle stimulating hormone (FSH), decreased anti-Müllerian hormone (AMH), oestradiol (E2) fluctuations, and long-term amenorrhea, which lead to an increased risk of a variety of diseases, such as female infertility, cardiovascular diseases, sexual dysfunction, diabetes mellitus type 2, and even early mortality [1]. POF is caused by factors, such as genetics, immunity, psychological factors, and chemotherapy injury, and the incidence of POF has increased in recent years. It was reported that chemotherapy agents are the most common causes of POF, and approximately 5% of cancer survivors who receive chemotherapy are young women [2]. Given the limitations of conventional hormone replacement therapy, it is necessary and urgent to develop effective therapeutic strategies, such as stem cell-derived therapies, to restore ovarian function in young women who suffer damage to chemotherapy [3].

Mesenchymal stem cells (MSCs) have been identified as a new frontier of therapeutic strategies to treat various disorders and damage, including POF [4]. MSCs are considered a promising source for cell therapies in regeneration medicine owing to their paracrine functions and directional differentiation [5]. A growing body of preclinical studies have noted that MSCs derived from human umbilical cord (hucMSC) and other adult tissues (adipose, skin, amniotic membrane, menstrual blood, placenta, and bone marrow) improve ovarian function and structure in POF models [4]. However, despite their exploration in preclinical studies, problems such as immunological rejection, cellular transplantation-related tumorigenicity and vascular embolization still limit the clinical application of MSCs [6].

There is an increasing amount of evidence indicating that the paracrine functions of MSCs typically rely on secreted extracellular vesicles to deliver biological factors to recipient cells [7]. Exosomes are a group of extracellular vesicles that can be transferred to recipient cells and functionally mediate remote communication, and they are considered an ideal noncell-based alternative for stem cell therapy [8]. Emerging evidence suggests that the major mechanism underlying the effects of MSC-based therapies in POF may be achieved by paracrine functions in immunomodulatory, proangiogenic and antiapoptotic effects in recipient cells instead of transdifferentiation into injured cells [5]. Our previous study also provided evidence that exosomes derived from hucMSCs (hucMSC-exosomes) exerted beneficial effects, including enhancing angiogenic potential, among rats with cisplatin-induced ovarian damage [9]. However, the therapeutic effect of hucMSC-derived exosomes needs to be further strengthened.

Previous studies have shown that hypoxia stimulates angiogenic behaviour in multiple pathophysiological processes [10]. It has also been shown that hypoxic preconditioning – a condition of low oxygen supply that may provide a better state for MSCs – is a suitable engineering approach to improve the therapeutic potential of MSCs in tissue regeneration applications [11]. It is generally believed that angiogenesis plays an important role in maintaining ovarian function and follicular development [12, 13]. Manipulation of ovarian angiogenesis represents a promising therapeutic strategy for POF treatment. However, the study of the relationship between hypoxia and ovarian angiogenesis is very limited, and it remains unclear whether exosomes derived from hypoxic preconditioning hucMSCs (hypoxic-hucMSC-exosomes, hypo-Exos) can obtain a better therapeutic efficacy than exosomes derived from normoxic environment cultured hucMSCs (normoxic-hucMSCs-exosomes, norm-Exos) in POF.

The present study aimed to explore whether hypoxic preconditioning can enhance the angiogenic potential of hucMSC-exosomes in experimental POF. In the current study, we isolated and characterized norm-Exos and hypo-Exos under normoxic or hypoxic conditions and thereby elucidated the biological function and underlying mechanism of hypo-Exos in angiogenesis activities by a series of angiogenesis-related assays in vitro. We also established a rat POF model via exposure to cisplatin to further explore the therapeutic potential and molecular mechanism underlying the beneficial effects of hypo-Exos in vivo. To the best of our knowledge, this is the first study to demonstrate that exosomes derived from hypoxia-conditionedhucMSCs strongly enhance angiogenesis via the transfer of miR-205-5p by targeting the phosphatase and tensin homolog (PTEN)/phosphoinositide 3-kinase (PI3K)/AKT/mammalian target of rapamycin (mTOR) signalling pathway. This study provides a theoretical basis and proposes a novel cell-free strategy for the treatment of POF with stem cell-derived products.

Materials and methods

Ethics statement

The experimental procedures were approved by the Ethics Committee of Qilu Hospital of Shandong University (approval number KYLL-202203-013). Human umbilical cords were obtained from informed consenting women delivered via normal vaginal delivery in Qilu Hospital of Shandong University and processed according to the principles expressed in the Declaration of Helsinki. All animal experimental protocols were approved by the Animal Care and Use Committee of Qilu Hospital of

Shandong University. All animal experiments were performed in strict compliance with the Guide for the Care and Use of Laboratory Animals.

Isolation and identification of hucMSCs

Primary hucMSCs were isolated from a fresh human umbilical cord according to the standard procedure we previously described [9, 14, 15]. After isolation, hucMSCs were maintained in alpha minimal essential medium (α-MEM, HyClone, USA) containing 10% foetal bovine serum (FBS, Gibco, USA) and 1% penicillin–streptomycin, grown in 5% CO_2 and 95% humidity at 37 °C and subcultured when they reached 80-90% confluence. The typical surface markers of hucMSCs were detected by flow cytometry using the following monoclonal antibodies: CD29, CD34, CD44, CD45, CD73, CD90, CD105, CD133, and CD146(1:1000, eBioscience, USA). Then, data were analysed using Flow Jo software. To test the multidirectional differentiation potential of hucMSCs, the cells were incubated with OriCell™ osteogenic, adipogenic, or chondrogenic differentiation media (Cyagen, China). The chondrogenic, adipogenic and osteogenic differentiation potential of hucMSCs was estimated with Alizarin Red staining, Oli Red O staining and Alcian Blue staining, respectively.

Isolation and identification of ROMECs

Rat ovarian microvascular endothelial cells (ROMECs) were isolated from fresh rat ovarian tissues using the Percoll density gradient centrifugation method based on the protocol described by Toshihiro Sakurai et al. [16]. The isolated cells were cultured in endothelial cell medium (ECM) supplemented with 5% FBS, 1% endothelial cell growth supplement, and 1% penicillin–streptomycin in 5% CO_2 and 95% humidity at 37 °C. ROMECs were detected by their cobblestone-like morphologic characteristics and CD31, CD34, and von Willebrand Factor (VWF) cell immunofluorescence staining as described [17].

Exposure of hucMSCs to hypoxia

To induce a hypoxic environment, hucMSCs were cultured in a humidified hypoxia modular incubator chamber at 37 °C with a hypoxic gas mixture composed of 5% O_2, 5% CO_2, and balanced N_2 for 24 h. The control hucMSCs were grown in a humidified incubator at 37 °C with 5% CO_2 under normoxic conditions of 21% O_2.

Purification of norm-exos and hypo-exos

After 72 h incubation of hucMSCs, the culture medium supernatant of 10^8 hucMSCs cultured in normoxic and hypoxic environments were collected for norm-Exo and hypo-Exo isolation, respectively. The culture medium supernatant was centrifuged at 1500 × g for 5 min and then 10,000 × g for 20 min at 4 °C to remove debris and apoptotic bodies. This step was followed by a repeated ultracentrifugation step at 120,000 × g for 70 min at 4 °C to purify exosomes. The final exosomal pellet was resuspended in phosphate-buffer saline (PBS) and then stored at -80 °C for subsequent experiments.

Characterization of norm-exos and hypo-exos

For exosome characterization, transmission electron microscopy (TEM; JEOL-1200EX, Japan) analysis was performed to visualize the appearance of freshly purified exosomes. Nanoparticle tracking analysis (NTA) was performed to detect the size distribution and mean diameter of exosomes by laser scattering microscopy (LSM, Zeta View® x30, Germany). Specific exosomal markersCalnexin, TSG101, CD9, CD63, and CD81(1:1000, Proteintech, China)were detected by western blotting. In addition, a bicinchoninic acid (BCA) protein assay was applied to evaluate the protein concentrations of exosomes.

Labelling and tracking of norm-exos and hypo-exos

To demonstrate the uptake of norm-Exos and hypo-Exos in ROMECs, exosomes were labelled with green fluorescent dye (PKH67). ROMECs were cocultured with norm-Exos and hypo-Exos at a concentration of 25 μg/mL for 12 h. Subsequently, the cells were fixed, counterstained with 4′,6-diamidino-2-phenylindole (DAPI), and observed using a fluorescence microscope.

EdU assay

EdU assays and colony formation assays were applied to assess cell proliferation under different conditions according to the standard protocol. For the EdU staining assay, the EdU Cell Proliferation Kit (RiboBio, China) was used to identify proliferative ROMECs following the manufacturer's procedures. ROMECs were cocultured with norm-Exos and hypo-Exos at a concentration of 25 μg/mL for 24 h. Nuclei were stained with DAPI, and the proliferation rate of ROMECs was assessed by calculating the number of EdU-positive cells under a fluorescence microscope.

Colony formation assay

For the colony formation assay, eight hundred ROMECs were seeded into each well of 6-well plates and treated with25 μg/mL norm-Exos or hypo-Exos at a concentration of for 24 h. for 7 days to allow colony growth. Cells were fixed with formaldehyde and stained with crystal violet. The number of colonies was counted manually, and the colonies were photographed.

Wound healing assay

Wound healing assays and Transwell assays were applied to assess cell migration under different conditions in accordance with methods reported in our previous studies [14]. For the wound healing assay, ROMECs were cultured in a 6-well plate. When cell confluence reached 90%, a scratch was made in the confluent monolayer using a pipette tip. The plates were washed to remove the debris and then incubated with 25 μg/mL norm-Exos and hypo-Exos for 24 h. The wound borders were photographed at 0 h and 24 h post-scratch using an inverted microscope.

Transwell migration assay

For the Transwell migration assay, ROMECs were counted and cultured in the upper chamber of the Transwell chamber (8.0-μm pore size, Corning, USA). After cocultured with norm-Exos and hypo-Exos at a concentration of 25 μg/mL in an incubator at 37 °C and 5% CO_2 for 24 h, the chamber was fixed with paraformaldehyde and stained with crystal violet. The cells that remained on the upper surface did not migrate and were removed, and those on the lower surface were visualized and imaged under an inverted microscope.

Tube formation assay

The formation of vessel-like structures was examined in a 24-well plate using an In Vitro Angiogenesis Assay Kit (Abcam, USA) following the manufacturer's instructions. ROMECs under different culture conditions were plated on extracellular matrix gels and incubated with 25 μg/mL norm-Exos or hypo-Exos at 37 °C for 12 h to allow tube formation. At the end of the cultivation, the tube network was stained with calcein acetoxymethyl, and the capillary-like structures were imaged using fluorescence microscopy. Additionally, the total tube length and tube number in three random fields were quantified as the tube formation ability.

miRNA high-throughput sequencing

Total RNA of exosomes was extracted from norm-Exos and hypo-Exos using TRIzol Reagent (Thermo Fisher, USA). RNA quantification was verified by a NanoDrop ND-1000, and RNA integrity and gDNA contamination were evaluated by denaturing agarose gel electrophoresis. The TruSeq Small RNA Sample Preparation Kit (Illumina, USA) was utilized to construct small RNA libraries. The samples were processed for deep sequencing using a MiSeq desktop sequencer system (Illumina, USA) according to the manufacturer's instructions. An adjusted P value < 0.05 and $|\log2(\text{fold change})| > 1$ indicated significantly differentially expressed genes. Prediction of downstream genes regulated by miRNAs was performed using microRNA Data Integration Portal (mirDIP), miRwalk, starBase, TargetScan, and miRDB.

Dual luciferase reporter assay

The binding sites between PTEN and miR-205-5p were predicted by a biological prediction website and further validated by the dual luciferase reporter assay. The mutant-type (MUT) 3′-UTR (MUT-PTEN) and wild-type (WT) 3′-UTR (WT-PTEN) were synthesized into the pmirGLO dual luciferase reporter vector (Promega, USA). Then, ROMECs were transfected with miR-205-5p NC or miR-205-5p mimic and later co-transfected with the two reporter plasmids according to our previously described protocol [18]. After 48 h, luciferase activities were measured using the Dual Luciferase® Reporter Assay System (Promega, USA) according to the manufacturer's instructions.

Establishment of the POF rat model

The work has been reported in line with the ARRIVE guidelines 2.0. Female Wistar rats weighing 170–190 g were obtained from Pengyue Laboratory Animal Co., Ltd. (Jinan, China) and raised in a pathogen-free environment. To establish the rat POF model, Wistar female rats were injected intraperitoneally with cisplatin for 14 days based on a protocol we described previously [9]. Cisplatin-induced POF rats were intravenously injected with a single dose of exosomes (400 μg dissolved in 200 μL PBS) obtained from different cell conditions under conscious state. and then equally and randomly divided into groups for different administration after modelling. The POF rats were weighed, and serum levels of follicle-stimulating hormone (FSH), oestradiol (E2), and Anti-Müllerian hormone (AMH) were detected by enzyme-linked immunosorbent assay (ELISA) at 0, 1, 2, and 4 weeks after exosome treatment. At the end of the study, these rats were euthanized by phenobarbitone and euthanized by carbon dioxide, and the ovaries were removed for subsequent experiments. The ovarian structure and follicle development in POF rats were determined by haematoxylin and eosin (HE) staining, proliferating cell nuclear antigen (PCNA) immunohistochemistry staining and terminal deoxynucleotidyl transferase dUTP nick end labelling (TUNEL) staining. The angiogenesis status of ovarian tissues in POF rats was determined using CD31 immunofluorescence staining.

Ovarian follicle counting and morphological analysis

The ovarian tissues were fixed with formalin, dehydrated in ethanol, cleared in xylene, embedded in paraffin, and sliced into 5-μm-thick sections. The slides were stained with HE using a Haematoxylin-Eosin Stain Kit (Solarbio, China) to detect ovarian morphology and follicle counts in accordance with the manufacturer's instructions. The

different categories of follicles, including atretic, primordial, primary, and secondary follicles, were counted by two investigators as described in the literature.

Immunohistochemical staining

For immunohistochemical staining, paraffin-embedded ovarian tissue sections were dewaxed in xylene, rehydrated through graded ethanol, heated in ethylenediaminetetraacetic acid (EDTA) solution, and blocked with bovine serum albumin (BSA). Next, slides were incubated with diluted PCNA primary antibody (1:500, Abcam, USA) followed by incubation with peroxidase-labelled secondary antibodies. PCNA-positive signals were finally observed with 3,3′-diaminobenzidine solution by counterstaining with haematoxylin reagent.

Immunofluorescence staining

For immunofluorescence staining, tissue samples from the in vivo experiment were blocked with 5% goat serum, incubated with diluted CD31 primary antibody (1:200, Abcam, USA), and stained with rhodamine–conjugated secondary antibodies. Next, tissues were counterstained with DAPI, and the stained sections were visualized by fluorescence microscopy to evaluate microvessel density in ovarian tissue. For cell immunofluorescence to identify primary ROMECs isolated from rat ovarian tissues, the antibodies used in this study were as follows: anti-VWF-FITC (1:100, Abcam, USA), anti-CD31 (1:200, Affinity, China) and anti-CD34 (1:200, Abcam, USA).

Western blotting

For western blot analysis, total protein from cell samples was isolated using radioimmunoprecipitation assay (RIPA) lysis buffer (Beyotime, China), and the protein concentration was measured by using a Bicinchoninic Acid (BCA) Protein Assay Kit (Beyotime, China). Proteins were separated by sodium dodecyl sulfate–polyacrylamide gel electrophoresis and transferred to polyvinylidene fluoride membranes (Millipore, USA). Then, the membranes were blocked with nonfat milk and incubated with primary antibodies. Next, membranes were incubated with horseradish peroxidase-conjugated secondary antibodies (1:2000, Proteintech, China). The resulting protein bands were visualized by the enhanced chemiluminescence detection system (Millipore, USA) The main antibodies used in this study are as follows: Calnexin (1:2000, Affinity, China), TSG101 (1:2000, Proteintech, China), CD9 (1:1000, Proteintech, China), CD63 (1:1000, Proteintech, China), CD81 (1:1000, Proteintech, China), GAPDH (1:5000, Proteintech, China), PTEN (1:2000, Affinity, China), PI3K (1:2000, Cell Signaling Technology, USA), p-PI3K (1:2000, Cell Signaling Technology, USA), AKT (1:2000, Cell Signaling Technology, USA), p-AKT (1:2000, Cell Signaling Technology, USA), mTOR (1:2000, Cell Signaling Technology, USA), and p-mTOR (1:2000, Cell Signaling Technology, USA).

Quantitative real-time polymerase chain reaction (qRT-PCR)

For qRT-PCR analysis, total RNA of cell or tissue samples was extracted using TRIzol Reagent (Thermo Fisher, USA). The cDNAs were synthesized by using a miScript II RT Kit (Qiagen, Germany), and then qRT−PCR was performed using a miScript SYBR Green PCR Kit (Qiagen, Germany) in a CFX96 Touch Real-Time PCR Detection System (Bio-Rad, USA) according to the manufacturer's instructions. miRNA and mRNA expression levels were calculated using the $2-\Delta\Delta Ct$ method with U6 and glyceraldehyde 3-phosphate dehydrogenase (GAPDH) as the endogenous controls.

Statistical analysis

Data are reported as the means±standard deviations (SD), and statistical analyses were performed using SPSS 22.0 software (SPSS, USA) and GraphPad Prism 6.0 software (GraphPad, USA). One-way analysis of variance (ANOVA) followed by Student-Newman−Keuls (SNK) test was applied to analyse variance among all groups. At least three biological replicates were performed for every experiment in this study, and a P value <0.05 was considered statistically significant in the present study.

Results

Identification and culture of hucMSCs and ROMECs

Primary hucMSCs were isolated from freshly isolated human umbilical cords as previously described by our lab [9, 14, 15]. Under the microscope, the cells adhered to the culture dish and exhibited a spindle-shaped, fibroblast-like morphology that is typical of MSCs (Fig. 1A). Under appropriate inductive conditions, MSCs differentiate into osteoblasts, adipocytes, and chondrocytes, as determined by Alizarin Red, Oli Red O, and Alcian Blue staining, respectively (Fig. 1B and D). Flow cytometry analysis was employed to demonstrate that hucMSCs were highly positive for classical MSC surface markers, including CD29, CD44, CD73, CD90, CD105, and CD166, but negative for CD34 and CD45 (Fig. 1E). For primary ROMECs isolated from fresh rat ovarian tissues, the isolated cells displayed a typical endothelial-like cobblestone morphology (Fig. 1F). Immunofluorescence staining showed that the isolated cells were highly positive for CD31, CD34, and VWF (Fig. 1G and I). Collectively, these results indicated that hucMSCs and ROMECs were successfully isolated and cultured.

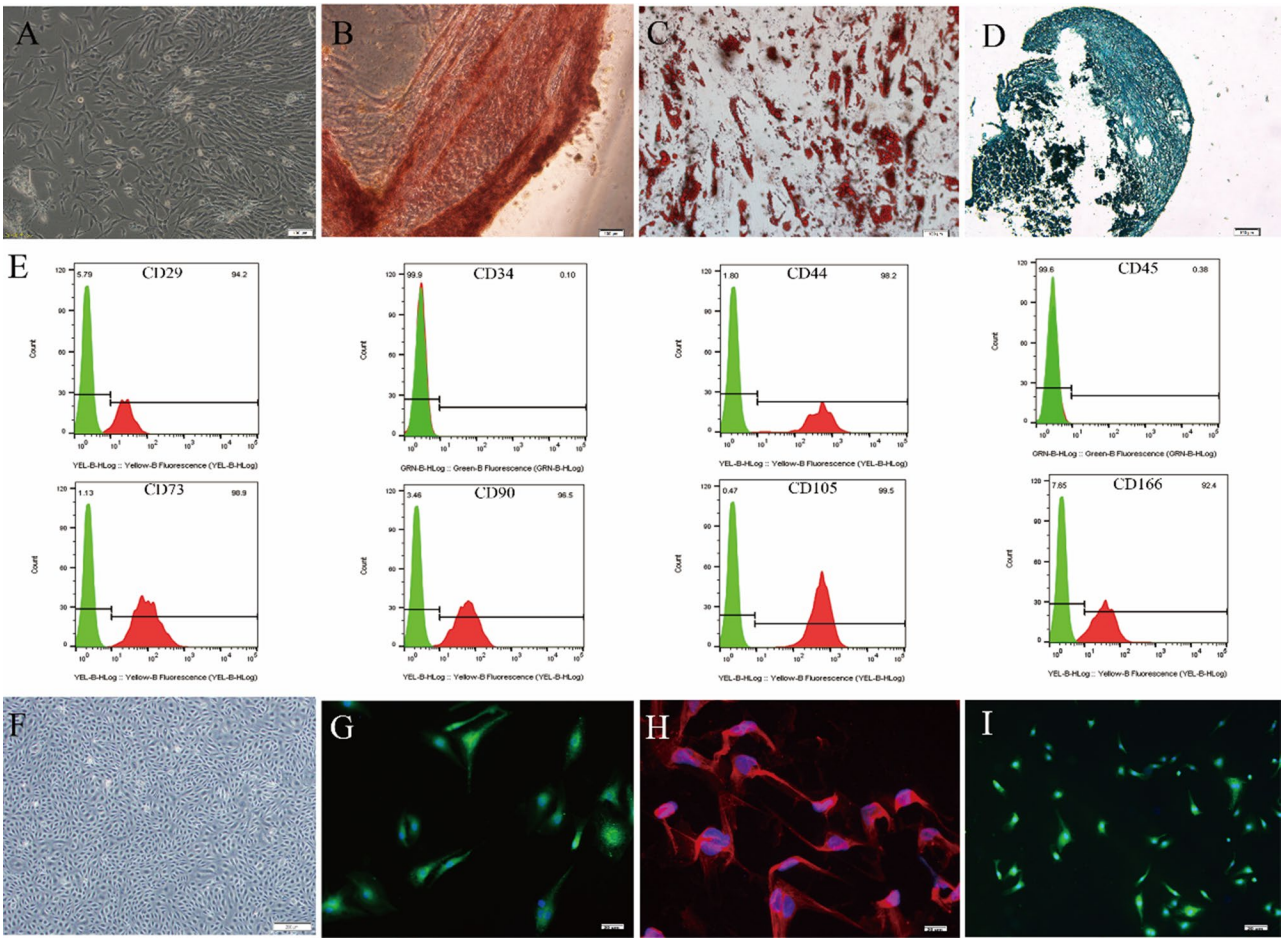

Fig. 1 Identification and culture of hucMSCs and ROMECs. **A**. Morphology of primary hucMSCs under a light microscope. **B**-**D**. Representative Alizarin Red, Oli Red O, and Alcian Blue staining images of chondrogenic, adipogenic and osteogenic differentiation of hucMSCs, respectively. **E**. hucMSC surface markers were determined by flow cytometry, $n = 3$ per group. **F**. Morphology of primary ROMECs under a light microscope. G-I. ROMECs were observed by cell immunofluorescence staining for CD31, CD34, and VWF

Hypoxic conditioning affected the content and function of exosomes from hucMSCs

Norm-Exos and hypo-Exos were isolated from hucMSCs under normoxic or hypoxic conditions via ultracentrifugation. These particles were characterized by western blotting, TEM analysis and NTA. TEM showed that the phenotypes of no n diameters (Fig. 2C). Western blotting results revealed that exosomal markers, including CD9, CD63, CD81 and TSG101, were present in both types of exosomes, and the negative exosome marker calnexin was not detected in either hucMSC-exosome type (Fig. 2D). TSG101, CD9, CD63, and CD81 protein levels were significantly increased in hypo-Exos compared with norm-Exos (Fig. 2E). In addition, the BCA protein assay results revealed that the exposure of hucMSCs to hypoxia induced significantly increased total protein concentrations of exosomes compared with cells cultured in normoxic conditions (Fig. 2F). To determine the potential biological functions of norm-Exos and hypo-Exos, we added exosomes labelled with the green fluorescent dye PKH67 to ROMECs. The results showed that both types of PHK67-labelled exosomes could be taken up by ROMEC and appeared in the cytoplasm around the nucleus (Fig. 2G). Interestingly, the rate of uptake in the hypo-Exo group was greater than that in the Norm-Exo group ($P<0.05$), suggesting that hypo-Exos are more easily taken up by ROMECs to produce effects on those cells (Fig. 2H). Consequently, all these results suggest that, compared to normoxic conditioning, hypoxia pretreatment affected the content and biological behaviour of exosomes from hucMSCs.

Hypoxic preconditioning enhances the angiogenic potential of hucmsc-exosomes in vitro

The biological performance of exosomes is affected by cell type and culture conditions [19]. To investigate the biological function of hypo-Exos in the angiogenic activities of endothelial cells, we cultured ROMECs with PBS, norm-Exos or hypo-Exos and performed a series of angiogenesis-related assays. We first detected the effects

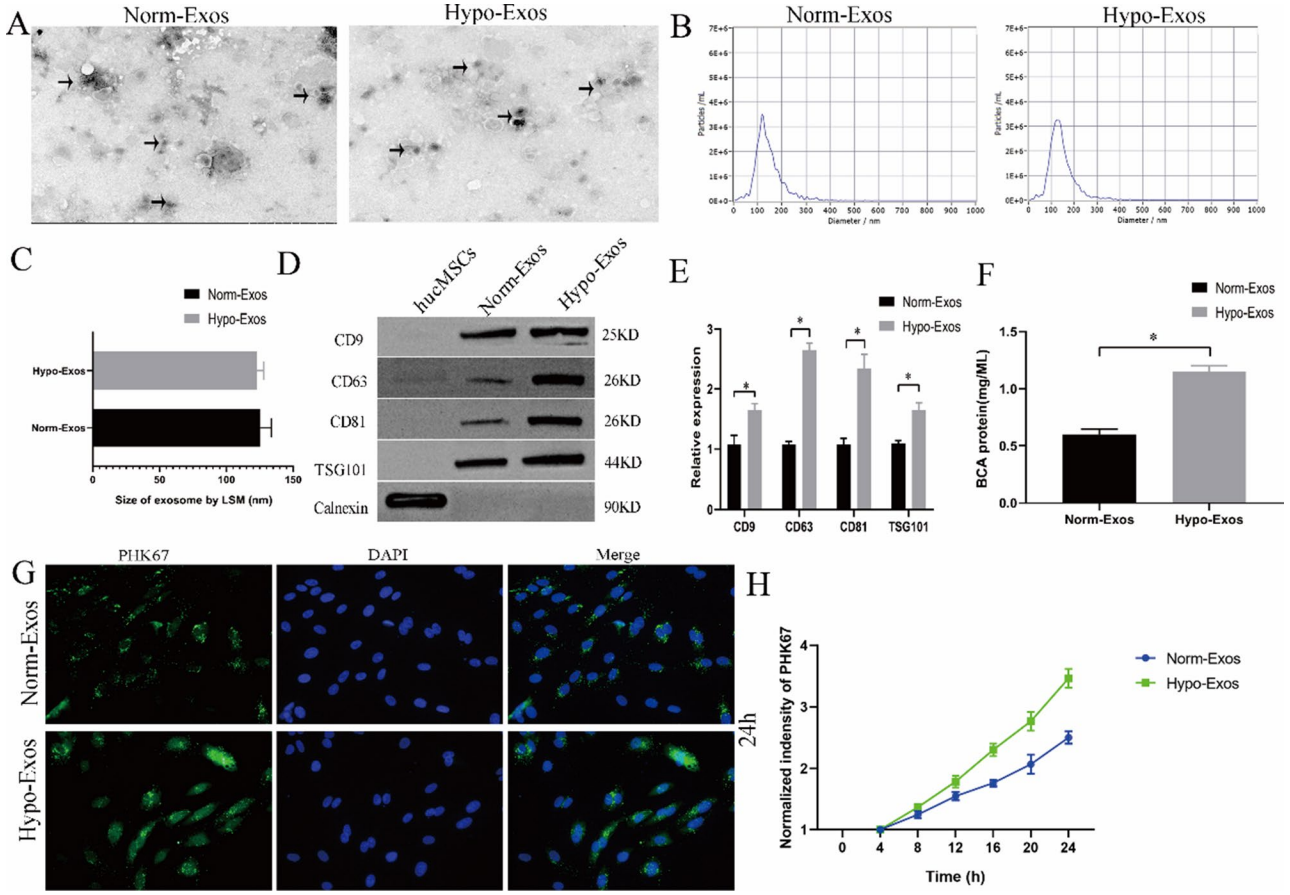

Fig. 2 Characterization and internalization of norm-Exos and hypo-Exos. **A**. Morphology of norm-Exos and hypo-Exos observed using TEM. **B**. Particle size distributions were determined by NTA. **C**. Comparison of the mean diameters of norm-Exos and hypo-Exos. **D**. The exosomal surface markers (TSG101, CD9, CD63, and CD81) in norm-Exos and hypo-Exos were assessed by western blotting. **E**. Semiquantitative analysis of the protein levels of TSG101, CD9, CD63, and CD81. **F**. Exosomal protein concentrations in norm-Exos and hypo-Exos were analysed using the BCA assay. **G**. Uptake of PKH67-labelled norm-Exos and hypo-Exos into ROMECs at 24 h. **H**. Statistical evaluation of fluorescence intensities in the norm-Exo and hypo-Exo groups. $n = 3$ per group, $^{*}P < 0.05$ for all figures

of hypo-Exos on the growth of ROMECs using the EdU assay and colony formation assay (Fig. 3A and B). The results showed that ROMEC proliferation was significantly increased in both the norm-Exos and hypo-Exos groups compared to the PBS group. However, ROMECs in the hypo-Exo group exhibited higher proliferation than those in the norm-Exo group (Fig. 3F and G). Moreover, scratch wound healing and Transwell assays were also conducted to assess the impact of hucMSC-exosomes on cell migration. Notably, the results showed that hypo-Exos had a much stronger stimulatory effect on the migration capability of ROMECs than norm-Exos (Fig. 3C, D and H, and 3I). We then investigated the effect of hypo-Exos on ROMEC angiogenesis using the tube formation assay. As expected, the results showed that incubation with hypo-Exos resulted in a greater increase in the total tube length and tube number of ROMECs than incubation with either PBS or norm-Exos (Fig. 3E, J and K). In addition, the qRT−PCR results showed that the mRNA expression of angiogenesis-promoting molecules insulin-like growth factor (IGF)-1, basic fibroblast growth factor (bFGF), transforming growth factor (TGF)-β, and vascular endothelial growth factors (VEGF)) was increased in the presence of either norm-Exos or hypo-Exos, and hypo-Exos significantly enhanced the gene expression of ROMECs compared to norm-Exos (Fig. 3L and O). In summary, we have provided compelling evidence that hypo-Exos significantly promote ROMEC proliferation, migration, and tube formation in vitro, demonstrating that hypoxic preconditioning enhances the angiogenic potential of hucMSC-exosomes in endothelial cells.

Hypoxic preconditioning strengthens the therapeutic angiogenesis effect of hucmsc-exosomes in a rat model of pof in vivo

Angiogenesis plays an important role in maintaining ovarian function and follicular development [12]. The manipulation of ovarian angiogenesis is a promising therapeutic strategy for POF treatment. To evaluate the

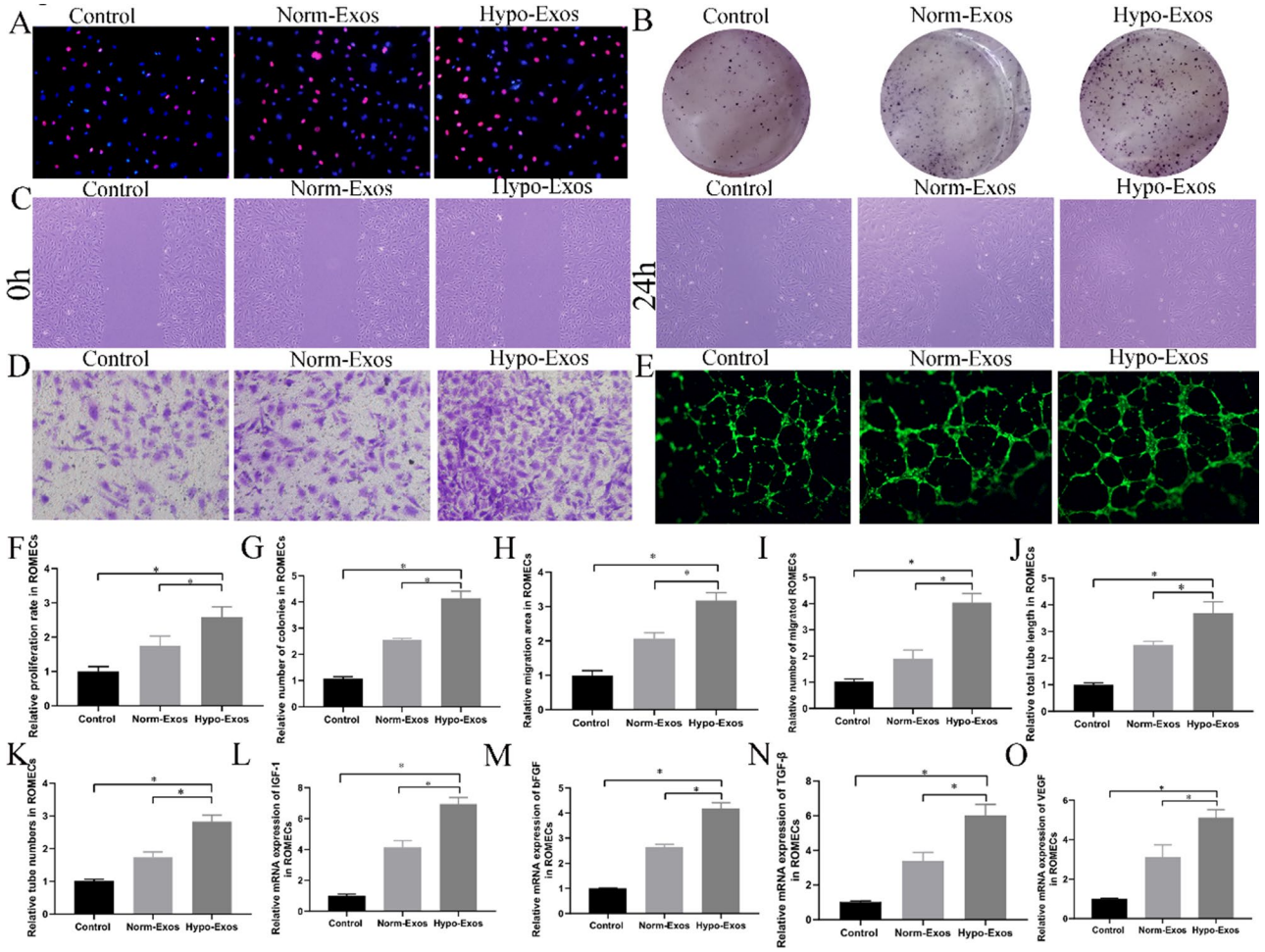

Fig. 3 Hypo-Exos significantly promoted ROMEC proliferation, migration, and tube formation and increased angiogenesis-promoting molecules in vitro. **A**. ROMEC proliferation was estimated by EdU assay, and representative images are shown. **B**. ROMEC proliferation was estimated by colony formation assay, and representative images are shown. **C**. ROMEC migration was estimated by scratch wound healing assay, and representative images are shown. **D**. ROMEC migration was estimated by transwell assay, and representative images are shown. **E**. ROMEC angiogenesis was estimated by colony formation assay, and representative images are shown. **F**. Quantification analysis of the colony formation numbers of ROMECs is shown. **G**. Quantification analysis of the proliferation rates of ROMECs is shown. **H**. Quantification analysis of the migration area of ROMECs is shown. **I**. Quantification analysis of the migrated cell numbers of ROMECs is shown. **J**. Quantification analysis of the total tube length of ROMECs is shown. **K**. Quantification analysis of the tube numbers of ROMECs is shown. L-O. qRT–PCR showed that the relative mRNA levels of angiogenesis-promoting molecules (IGF-1, bFGF, TGF-β, and VEGF) were obviously increased in the hypo-Exos group than in the norm-Exos and PBS groups. $n = 3$ per group, $^*P < 0.05$ for all figures

therapeutic effect of hypo-Exos on ovarian function and angiogenesis in POF in vivo, rats with chemotherapy-induced ovarian damage were injected with PBS, norm-Exos or hypo-Exos via the caudal vein after 14 days [9]. We found that the body weight and the levels of E2 and AMH in POF rats were significantly increased in the norm-Exo group and hypo-Exo group compared with the PBS group without exosome treatment, whereas FSH levels were significantly decreased starting from the first week after exosome treatment. However, more importantly, hypo-Exos exhibited a much stronger stimulatory effect in maintaining body weight and improving E2 and AMH levels expression than norm-Exos (Fig. 4A and D). The principal pathophysiological mechanism of POF is granulosa cell (GC) apoptosis and follicular atresia. Herein, we performed HE staining to observe the morphologic structure of the ovarian tissues. The results showed that the different categories of follicles, including atretic, primordial, primary, and secondary follicles, were increased in the norm-Exo group and hypo-Exo group compared to the PBS group (Fig. 4E and F). Moreover, the follicle counts were higher in the hypo-Exo group compared with the norm-Exo group. Subsequently, we further evaluated cell proliferation and apoptosis in developing follicles and antral follicles by PCNA immunohistochemistry and TUNEL staining. Consistent with the morphological results, PCNA immunohistochemistry staining results showed that administration of hypo-Exos to POF rats increased proliferating cells in ovarian tissue compared to norm-Exo treatment or PBS

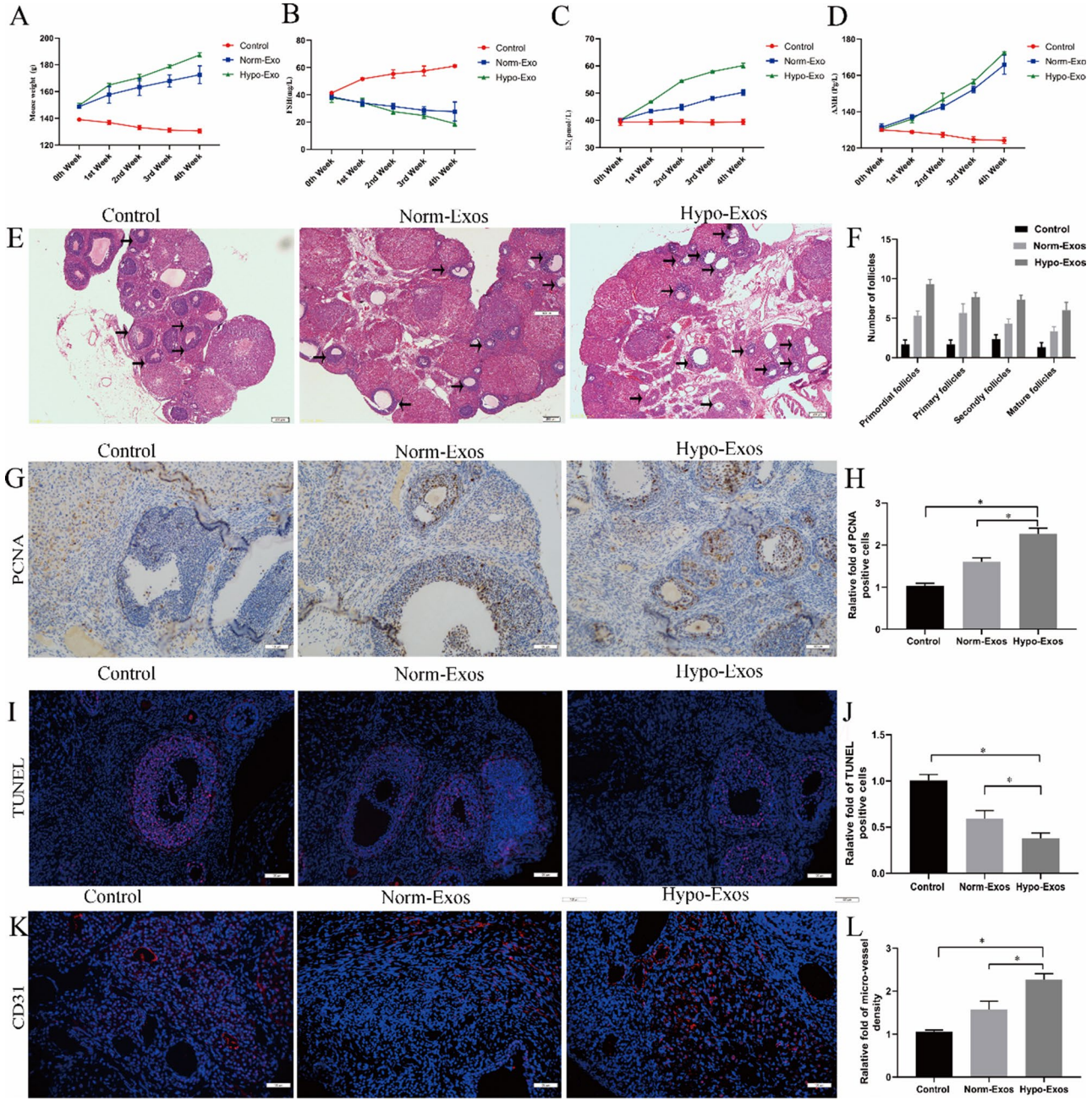

Fig. 4 Hypoxia pretreatment strengthens the therapeutic angiogenesis effect of hucMSC-exosomes in a rat model of POF in vivo. The POF rats were injected with PBS, norm-Exos and hypo-Exos via the caudal vein. The weights of the rats were measured, and FSH, E2, and AMH serum levels were estimated by ELISA at 0, 1, 2, 3 and 4 weeks after intervention. Histopathological examination of ovarian tissues was performed 4 weeks after treatment. **A**. The change in body weight was observed in each group. **B**. The change in FSH serum levels was observed in each group. **C**. The change in E2 serum levels was observed in each group. **D**. The change in AMH serum levels was observed in each group. **E**. HE-stained ovarian sections of POF rats showing the morphologic structure of the ovarian tissues. **F**. The different developmental stages of follicles were assessed and are shown. **G**. Representative photomicrographs of PCNA immunohistochemistry staining in ovarian tissues of three groups 28 days after interventions. **H**. Quantitative analysis of PCNA-positive cells in ovarian tissues. I. Representative photomicrographs of TUNEL staining in ovarian tissues of three groups 28 days after interventions. **J**. Quantitative analysis of TUNEL-positive cells in ovarian tissues. **K**. Representative photomicrographs of CD31 immunofluorescence staining in ovarian tissues of three groups 28 days after interventions. **L**. Quantitative analysis of blood vessel density in ovarian tissues. $^{*}P < 0.05$ for all figures. $n = 10$ for each group

treatment (Fig. 4G and H). In addition, TUNEL staining results verified that hypo-Exos significantly inhibited chemotherapy-induced apoptosis of GCs in ovarian tissue compared to norm-Exos and PBS (Fig. 4I and J). In short, the above results revealed that hypo-Exos can more effectively repair damaged ovarian structures and improve ovarian function in POF rats. Next, ovarian vascularization in POF rats was analysed by CD31 immunofluorescence staining. Consistently, both the hypo-Exo group and norm-Exo group showed a significant increase in microvessel density in ovarian tissue compared to the PBS group ($P<0.05$). Moreover, POF rats treated with hypo-Exos exhibited a stronger microvessel density than those treated with norm-Exos (Fig. 4K and L). Together, our results clearly suggest that hypo-Exos could restore ovarian function by enhancing ovarian angiogenesis in a rat model of POF, further demonstrating that hypoxia pretreatment further strengthens the therapeutic angiogenesis effect of hucMSC-exosomes in vivo.

miR-205-5p is upregulated in hypo-exos and can be transferred to ROMECs

Exosomes serve as crucial regulators of cell-to-cell communication, and their effects mainly depend on their internal contents [20, 21]. miRNAs, which are indispensable components that are selectively packaged into exosomes, play a crucial role in the biological behaviour modulation of target cells [22]. To identify the potential molecular mechanism responsible for the angiogenesis modulation of hypo-Exos in vitro and in vivo, high-throughput miRNA sequencing of norm-Exos and hypo-Exos was performed. The differential expression profiles of miRNAs between norm-Exos and hypo-Exos are described in the heatmap and scatter plot analysis (Fig. 5A and B). Based on our exosomal miRNA sequencing results, we further validated the expression levels of the top six upregulated miRNAs by qRT−PCR: miR-149-3p, miR-149-5p, miR-185-3p, miR-205-5p, miR-432-5p, and miR-939-3p (Fig. 5C). We next searched the literature to examine candidate miR-205-5p, which exhibited the most significantly increased expression in hypo-Exos and has been reported to be involved in angiogenesis [23]. Kyoto Encyclopedia of Genes and Genomes (KEGG) analysis revealed that miR-205-5p participated in the PI3K-AKT signalling pathway (Fig. 5D). In addition, qRT−PCR data confirmed that the levels of miR-205-5p were significantly increased in the ROMECs after treatment with hypo-Exos (Fig. 5E). Therefore, miR-205-5p was selected for further study.

To determine whether exosomal miR-205-5p can play a role in the regulation of ROMEC function, we first constructed miR-205-5p-overexpressing normoxic-hucMSCs (miR-205-5p^{OE}-normoxic-hucMSCs) and miR-205-5p-knockdown

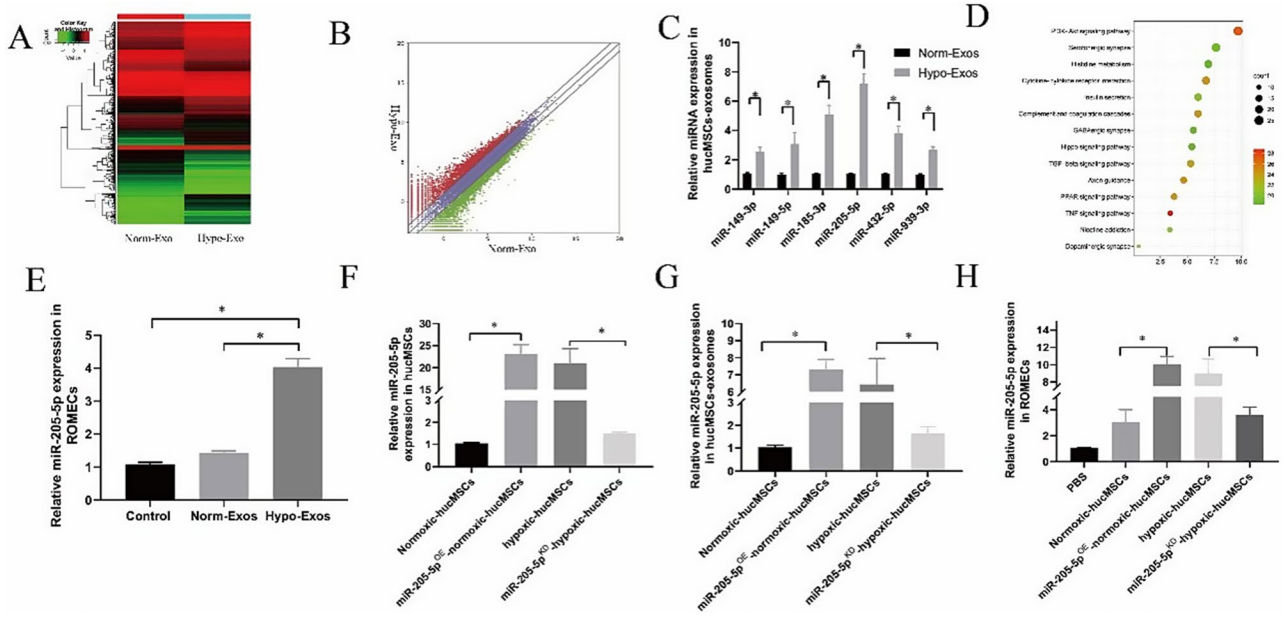

Fig. 5 miR-205-5p is upregulated in hypo-Exos and can be transferred to ROMECs. **A**. Heatmap of upregulated and downregulated miRNAs in norm-Exos and hypo-Exos. **B**. Scatter plot of upregulated and downregulated miRNAs in hypo-Exos and norm-Exos. **C**. Verification of the top six elevated miRNAs between norm-Exos and hypo-Exos by qRT–PCR. D. KEGG analysis of miR-205-5p was performed, and the enrichment map is shown. **E**. miR-205-5p expression in the ROMECs was significantly increased after the administration of hypo-Exos. **F**. The lentiviral vector transfection-mediated upregulation and downregulation of miR-205-5p expression was verified by qRT–PCR. **G**. miR-205-5p expression in miR-205-5pKD-hypo-Exos and miR-205-5pOE-norm-Exos. **H**. miR-205-5p expression in ROMECs after treatment with miR-205-5pKD-hypo-Exos and miR-205-5pOE-norm-Exos. *$P<0.05$ for all figures, $n=3$ for each group

hypoxic-hucMSCs (miR-205-5p^{KD}-hypoxic-hucMSCs) using a lentiviral-based method as previously reported [15]. The lentiviral vector transfection in hucMSCs was verified by qRT−PCR (Fig. 5F). We also confirmed that exosomal miR-205-5p expression was decreased in miR-205-5p^{KD}-hypo-Exos and increased in miR-205-5p^{OE}-norm-Exos compared with hypo-Exos and norm-Exos, respectively (Fig. 5G). More importantly, similar results of miR-205-5p expression were found in target ROMECs after treatment with miR-205-5p^{KD}-hypo-Exos and miR-205-5p^{OE}-norm-Exos (Fig. 5H). Taken together, these results provide evidence that exosomal miR-205-5p can be transferred to ROMECs and that miR-205-5p might play a crucial role in the regulation of ROMEC function by hypo-Exos, which requires further study.

Hypoxia pretreatment enhances the angiogenic potential of hucMSC-exosomes via the transfer of miR-205-5p in vitro and in vivo

Our in vitro and in vivo analyses indicated that hypo-Exos enhance angiogenesis compared to norm-Exos. To study the effects of exosomal miR-205-5p on the regulation of ROMEC function by hucMSC-exosomes, we conducted a series of angiogenesis-related assays using gain and loss strategies in vitro (supplementary Fig. 1A-E). Proliferation and migration assay results showed that overexpression of miR-205-5p expression by miR-205-5p^{OE}-norm-Exos significantly increased ROMEC proliferative and migratory activities in vitro compared to norm-Exos, and knockdown of miR-205-5p expression by miR-205-5p^{KD}-hypo-Exos impaired cell proliferative and migratory activities compared to hypo-Exos (Fig. 6A and D). Furthermore, the tube formation ability of ROMECs was significantly enhanced by miR-205-5p^{OE}-norm-Exo treatment but weakened by miR-205-5p^{KD}-hypo-Exo compared to the corresponding controls (Fig. 6E and F). Moreover, the expression levels of angiogenesis-related genes (IGF-1, bFGF, TGF-β, and VEGF) were considerably increased in miR-205-5p^{OE}-norm-Exo-treated ROMECs and reduced in miR-205-5p^{KD}-hypo-Exo-treated ROMECs compared with the corresponding controls (Fig. 6G and J).

Next, we further validated the role of exosomal miR-205-5p in hypo-Exo-induced angiogenesis in a rat POF model. We found that the body weight and E2 and AMH levels were higher in the miR-205-5p^{OE}-norm-Exo group compared with the norm-Exo group, and FSH levels exhibited an opposite trend compared with E2 and AMH levels. Significant decreases in body weight and E2 and AMH levels were observed in the miR-205-5p^{KD}-hypo-Exo group compared with the hypo-Exo group, and FSH levels exhibited an opposite trend compared with E2 and AMH levels (Fig. 6K and N). PCNA immunohistochemistry and TUNEL staining results showed that miR-205-5p^{OE}-norm-Exo treatment in POF rats increased proliferating cells but decreased the apoptotic rate in ovarian tissue compared to hypo-Exo treatment (Fig. 6O and P, supplementary Fig. 2A-C). The above mentioned results indicated that miR-205-5p in hucMSC-exosomes can restore ovarian function more effectively in rats with chemotherapyinduced ovarian damage. Furthermore, based on CD31 immunofluorescence staining, we found that the micro-vessel density in the ovarian tissue of POF rats was significantly enhanced by miR-205-5p^{OE}-norm-Exo treatment but weakened by miR-205-5p^{KD}-hypo-Exo treatment (Fig. 6Q, supplementary Fig. 2D). Overall, both our in vitro and in vivo results suggested that hypo-Exos enhance endothelial function and angiogenesis via the transfer of miR-205-5p.

PTEN is a direct target of miR-205-5p

To elucidate the potential target regulated by miR-205-5p in ROMECs, online databases (mirDIP, miRwalk, starBase, TargetScan, and miRDB) were used to predict the potential target genes of miR-205-5p in ROMECs. A Venn diagram of the predicted target genes was plotted, and we detected 6 candidate target genes in the intersection of the predicted results (Fig. 7A). Among them, PTEN, a tumour suppressor gene that regulates normal vascular development and tumour angiogenesis [24, 25], was hypothesised to be the most likely predicted target of miR-205-5p. qRT−PCR results verified that PTEN was the most downregulated among these genes (Fig. 7B). It was found that miR-205-5p and PTEN possessed a potential binding site (Fig. 7C). To further confirm whether miR-205-5p targets PTEN in ROMECs, we first performed a dual-luciferase reporter assay as previously described [18]. The results showed that miR-205-5p mimics markedly reduced the luciferase activity of cells in the PTEN-WT group (Fig. 7D), but the miR-205-5p inhibitor markedly increased the luciferase activity (Fig. 7E). No significant difference in the PTEN-MUT group was observed. Then, we further determined PTEN expression levels by qRT−PCR and western blotting. qRT−PCR and western blotting demonstrated that miR-205-5p mimics markedly decreased the mRNA and protein expression of PTEN in ROMECs. In contrast, the opposite effect on PTEN expression levels was observed when miR-205-5p expression was downregulated by miR-205-5p inhibitors (Fig. 7F and H). The above results indicated that PTEN is a downstream target of miR-205-5p in ROMECs.

Exosomal miR-205-5p enhances angiogenesis by targeting PTEN

PTEN has been implicated in the suppression of tumorigenesis and angiogenesis [24, 25]. However, its role in ROMECs has never been systematically elaborated. We further confirmed the functions of PTEN expression

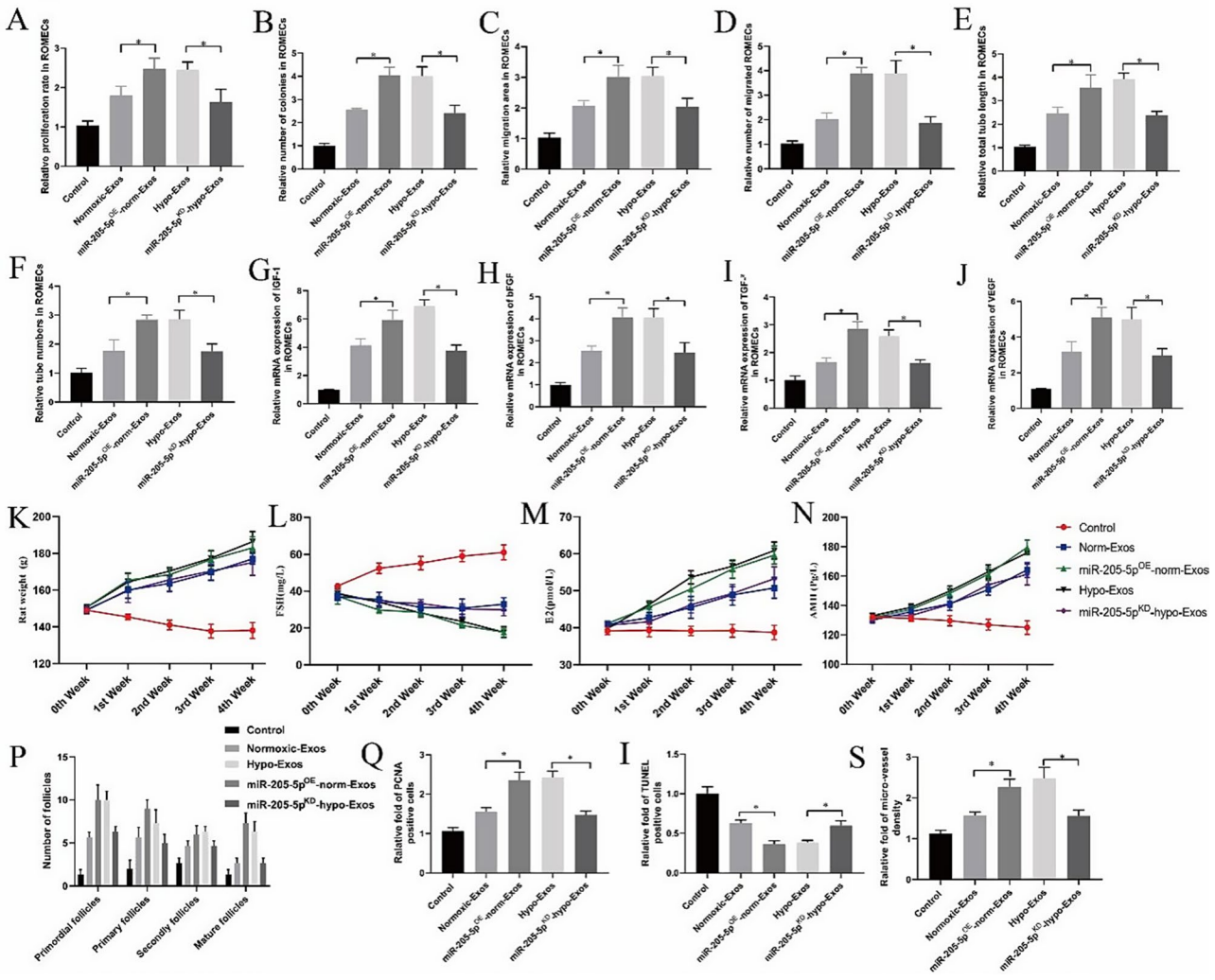

Fig. 6 Hypoxia pretreatment enhances the angiogenic potential of hucMSC-exosomes via transfer of miR-205-5p in vitro and in vivo. **A**-**D**. Quantitative analysis of the proliferative and migratory capacities of ROMECs after treatment with miR-205-5p^{KD}-hypo-Exos or miR-205-5p^{OE}-norm-Exos. **E**-**F**. Quantitative analysis of the tube formation ability of ROMECs after treatment with miR-205-5p^{KD}-hypo-Exos or miR-205-5p^{OE}-norm-Exos. **G**-**J**. The relative expression of angiogenesis-promoting molecules (IGF-1, bFGF, TGF-β, and VEGF) in ROMECs after treatment with miR-205-5p^{KD}-hypo-Exos or miR-205-5pOE-norm-Exos. **K**. Body weight of POF rats after treatment with miR-205-5p^{KD}-hypo-Exos and miR-205-5p^{OE}-norm-Exos. **L**-**N**. FSH, E2, and AMH serum levels in POF rats after treatment with miR-205-5p^{KD}-hypo-Exos or miR-205-5p^{OE}-norm-Exos. **O**. Quantitative analysis of PCNA-positive cells in POF rats after treatment with miR-205-5p^{KD}-hypo-Exos or miR-205-5p^{OE}-norm-Exos. **P**. Quantitative analysis of TUNEL-positive cells in POF rats after treatment with miR-205-5p^{KD}-hypo-Exos or miR-205-5p^{OE}-norm-Exos. **Q**. Quantitative analysis of blood vessel density in POF rats after treatment with miR-205-5p^{KD}-hypo-Exos or miR-205-5p^{OE}-norm-Exos. *$P < 0.05$ for all figures. $n = 10$ for each group

in the angiogenic activities of ROMECs in this study. ROMECs were transfected with PTEN siRNA and pcDNA-PTEN. As expected, we found that knockdown of PTEN expression by PTEN siRNA enhanced cell proliferation and migration, whereas upregulation of PTEN expression by pcDNA-PTEN inhibited cell proliferation and migration (Fig. 8A and D, supplementary Fig. 3A-D). Similar results were obtained regarding the influence of PTEN siRNA and pcDNA-PTEN on the tube formation ability of ROMECs (Fig. 8E-F, supplementary Fig. 3E). Furthermore, the expression levels of angiogenesis-related genes (IGF-1, bFGF, TGF-β, and VEGF) were considerably increased in PTEN siRNA-treated ROMECs and lower in pcDNA-PTEN-treated ROMECs than in the corresponding controls (Fig. 8G and J). Additionally, we examined the role of exosomal miR-205-mediated inhibition of PTEN in ROMECs. The qRT−PCR and western blotting results revealed that the PTEN mRNA and protein levels in hypo-Exo-treated ROMECs were lower than those in norm-Exos, whereas knockdown of miR-205-5p in hypo-Exos by miR-205-5p^{KD}-hypo-Exos effectively reversed the PTEN expression induced by administration of hypo-Exos (Fig. 8K and M). These results further

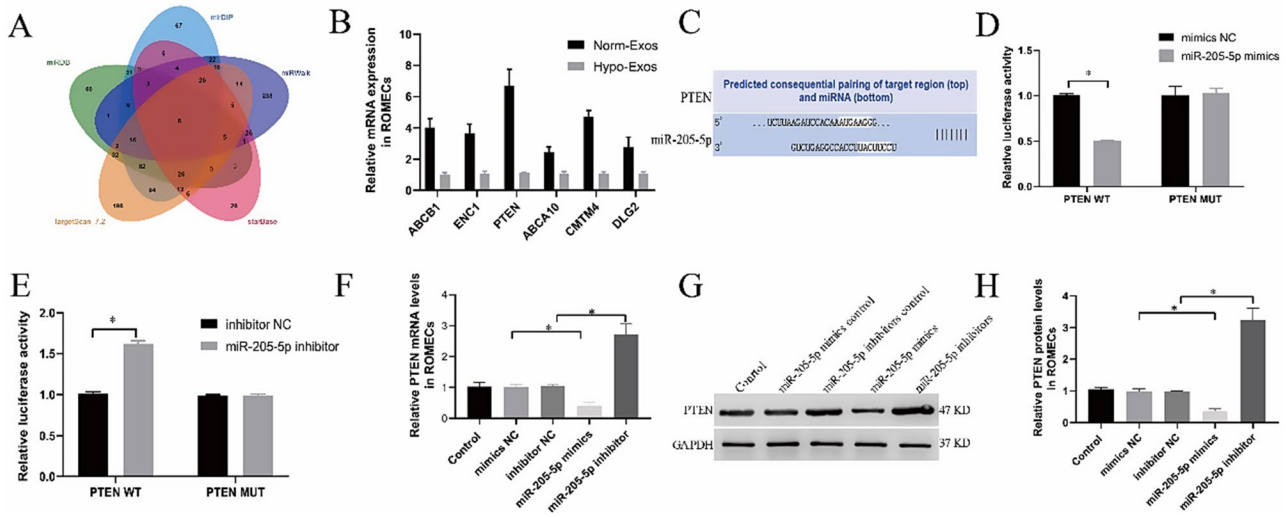

Fig. 7 PTEN is a direct target of miR-205-5p. **A**. The targets of miR-205-5p were predicted using four different miRNA target databases (miRanda, TargetScan, miRBase, and miRDB). **B**. qRT–PCR results verified that PTEN was most downregulated among these genes. **C**. The prediction of binding sites between miR-205-5p and PTEN. **D**-**E**. The combination of PTEN and miR-205-5p was detected by dual-luciferase reporter assay. **F**. Quantitation of PTEN mRNA expression in the cells of each group after treatment with miR-205-5p mimics or inhibitors or their corresponding controls as measured by qRT–PCR. **G**. PTEN protein expression in cells of each group after treatment with miR-205-5p mimics or inhibitors or their corresponding controls as detected by Western blotting. **H**. Semiquantitative analysis of PTEN protein levels. *$P < 0.05$ for all figures, $n = 3$ for each group

demonstrated that exosomal miR-205-5p enhances angiogenesis by targeting PTEN in ROMECs.

The PI3K/AKT/mTOR signalling pathway is involved in hypo-Exo-induced angiogenesis enhancement

The PI3K/AKT/mTOR pathway plays a crucial role in regulating angiogenesis [26]. KEGG analysis and previous research indicated that PTEN is involved in the PI3K-AKT signalling pathway [25, 27]. Therefore, we explored whether the proangiogenic effects of hypo-Exos were due to PTEN-mediated PI3K/AKT/mTOR activation in ROMECs (Fig. 8N). Western blotting results showed that hypo-Exo treatment resulted in increased levels of p-AKT, p-mTOR and p-PI3K compared to norm-Exo and PBS treatment in ROMECs. After treatment with miR-205-5p^{KD}-hypo-Exos, p-AKT, p-mTOR and p-PI3K expression levels in ROMECs all showed a decreasing trend compared to hypo-Exos (Fig. 8O and Q). As expected, after treatment with miR-205-5pOE-norm-Exos, p-AKT, p-mTOR and p-PI3K expression levels in ROMECs all showed an increasing trend compared to norm-Exos (Fig. 8O and Q). In the end, we conclude that the trend of p-AKT, p-mTOR and p-PI3K expression was contrary to that noted for PTEN. However, AKT, mTOR and PI3K expression levels were relatively stable in ROMECs. Taken together, our results indicated that exosomes derived from hypoxia-conditioned hucMSCs strongly enhance angiogenesis via the transfer of miR-205-5p by targeting the PTEN/PI3K/AKT/mTOR signalling pathway(Fig. 9).

Discussion

The occurrence of POF in women who receive chemotherapy represents an intractable medical problem [28]. The incidence of POF has increased in recent years, and the clinical effect of conventional treatment methods is limited, which makes it necessary and urgent to develop a new medicine and strategy for the treatment of POF. In this paper, for the first time, we provide in vitro and in vivo evidence that hypoxic preconditioning enhances the angiogenic potential of hucMSC-exosomes in experimental POF. Further mechanistic studies showed that hypo-Exos enhance endothelial function and angiogenesis via the transfer of miR-205-5p by targeting the PTEN/PI3K/AKT/mTOR signalling pathway. Overall, our research highlights the therapeutic prospects and mechanisms of hypo-Exos for the clinical treatment of POF.

During the past decade, numerous studies have shown that MSCs represent an appealing therapeutic approach for POF [4, 5]. Emerging evidence suggests that the therapeutic potential of MSCs is largely dependent on their secreted exosomes as vehicles of proteins, RNA, and other bioactive molecules [7, 8]. In our previous study, we reported that hucMSC-exosomes exerted anti-apoptotic and pro-angiogenic effects in rats with cisplatin-induced ovarian damage [9]. Increasing evidence has shown that the therapeutic efficacy of MSC-exosomes is highly dependent on the physiological or pathological state of MSCs [29]. Researchers have spent considerable energy and financial resources to obtain better effects of exosomes. Therefore, we envisaged that hucMSC-exosomes, as natural therapeutic delivery vehicles, could be

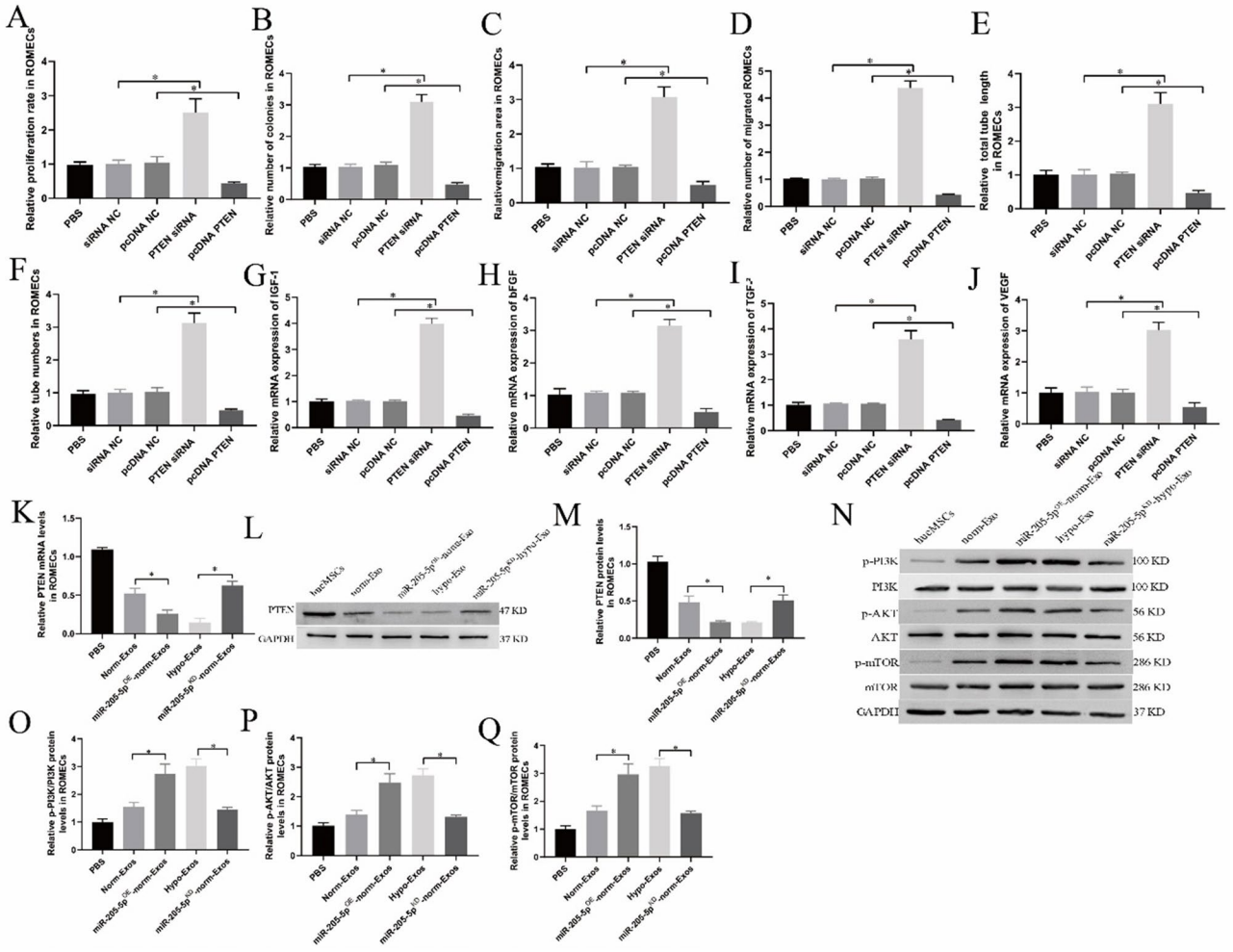

Fig. 8 The PTEN/PI3K/AKT/mTOR signalling pathway is involved in hypo-Exo-induced angiogenesis enhancement. **A**-**D**. Quantitative analysis of the proliferative and migratory capacities of ROMECs after transfection with PTEN siRNA or pcDNA-PTEN. **E**-**F**. Quantitative analysis of the tube formation ability of ROMECs after transfection with PTEN siRNA or pcDNA-PTEN. **G-J**. The relative mRNA expression of angiogenesis-promoting molecules (IGF-1, bFGF, TGF-β, and VEGF) in ROMECs after transfection with PTEN siRNA or pcDNA-PTEN. **K**. Quantitative analysis of PTEN mRNA expression in ROMECs after transfection with PTEN siRNA or pcDNA-PTEN or their corresponding controls as measured by qRT–PCR. **L**. PTEN protein expression in ROMECs after transfection with PTEN siRNA or pcDNA-PTEN or their corresponding controls as detected by western blotting. M. Semiquantitative analysis of PTEN protein levels. **N**. Western blotting was performed to evaluate the PI3K/AKT/mTOR signalling pathway. **O**. Semiquantitative analysis of p-AKT protein expression. **P**. Semiquantitative analysis of p-mTOR protein expression. **Q**. Semiquantitative analysis of p-PI3K protein expression. $^{*}P < 0.05$ for all figures. $n = 3$ for each group

engineered to strengthen their therapeutic potential in POF.

In this study, primary hucMSCs were isolated and identified from freshly isolated human umbilical cords given the numerous advantages provided over other adult MSCs. For example, these cells are free from ethical complications, exhibit and earlier embryologic phase, are obtained from noninvasive procedures, and are amenable to large-scale expansion [8, 30]. Currently available data indicate that MSCs are generally exposed to normoxic conditions (21% O_2) during in vitro culture. Correspondingly, the oxygen level in the body ranges from 1 to 12% under physiological conditions [23]. Studies have also shown that short-term exposure of MSCs to hypoxia not only enhances the proliferation and genetic stability of MSCs but also changes the content and function of exosomes [31, 32]. Hypoxic preconditioning has been extensively studied in many types of disease models and exhibits therapeutic potential in myocardial infarction, spinal cord injury, and diabetic wounds [11, 33–35]. The present study was performed to explore whether hypoxic preconditioning can enhance the angiogenic potential of exosomes derived from hypoxia-conditioned hucMSCs in experimental POF.

Previous studies have clarified that endothelial cell proliferation, migration, and tube formation are principal characteristics involved in angiogenesis [26]. In this study, we provided compelling evidence that hypo-Exos significantly promote ROMEC proliferation, migration, and tube formation in vitro, demonstrating that hypoxic

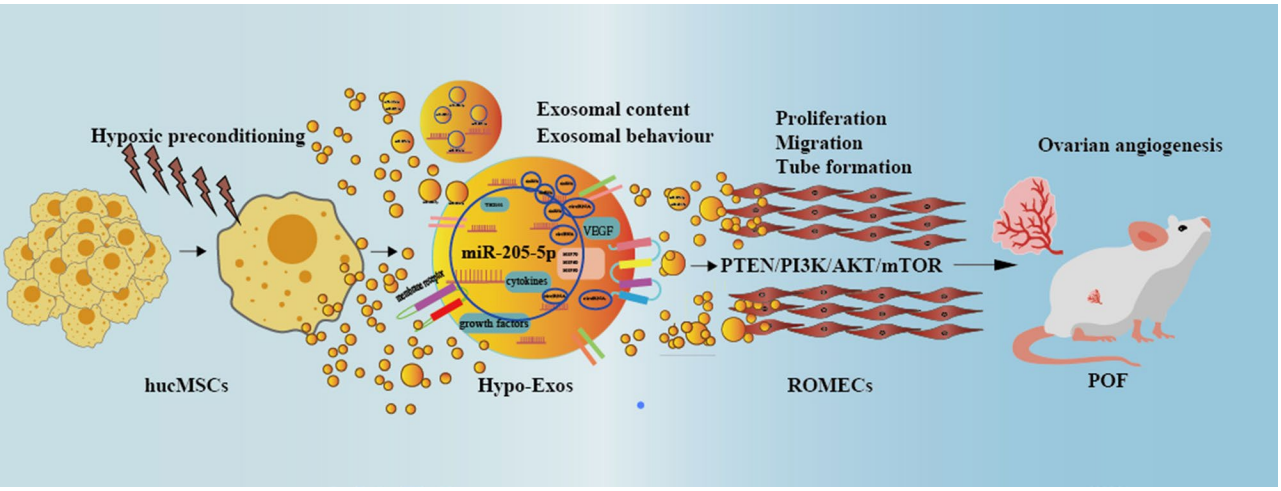

Fig. 9 A schematic diagram of hypoxia-conditioned hucMSCs enhancing angiogenesis via the transfer of miR-205-5p by targeting the PTEN/PI3K/AKT/mTOR signalling pathway

preconditioning enhances the angiogenic potential of hucMSC-exosomes in endothelial cells. A great deal of researches showed that angiogenesis plays an important role in maintaining ovarian function and follicular development. The manipulation of ovarian angiogenesis represent a promising therapeutic strategy for POF treatment [12, 13]. It is generally believed that ROMECs exhibited a different phenotypic and functional characteristic compared with the other tissue-source origin endothelial cells. Therefore, ROMECs were isolated and identified from rat ovarian to established in vitro POF model.To evaluate the therapeutic effect of hypo-Exos on ovarian function and angiogenesis in POF in vivo, we also established a cisplatin-induced rat POF model as we previously described. Our study showed that hypo-Exos could restore ovarian function by enhancing ovarian angiogenesis in a rat model of POF, which demonstrated that hypoxia pretreatment further strengthened the therapeutic angiogenesis effect of hucMSC-exosomes in vivo.

It is generally accepted that exosomes serve as crucial regulators of cell-to-cell communication, and this function mainly depends on their internal contents [20, 21]. miRNAs, which are indispensable components that are selectively packaged into exosomes, play a crucial role in the biological behaviour modulation of target cells [22]. In this research, we also identified the potential molecular mechanism responsible for the angiogenesis modulation of hypo-Exos in vitro and in vivo. With the help of miRNA high-throughput miRNA sequencing, qRT-PCR analysis, and western blotting, we identified that hypo-Exos enhance endothelial function and angiogenesis via the transfer of miR-205-5p in vitro and in vivo. In this study, we chose miR-205-5p as a candidate miRNA not only according to the miRNA sequencing data and KEGG pathway enrichment analysis but also based on evidence indicating that miR-205-5p is involved in angiogenesis [29]. Based on the results of bioinformatics analysis, dual luciferase reporter assays, and gain- and loss-of-function studies, we confirmed that PTEN is a downstream target of miR-205-5p in ROMECs. Among numerous genes, PTEN was selected for further exploration because it has been reported to play a role in the suppression of tumorigenesis and angiogenesis. Additionally, we focused on the PI3K/AKT/mTOR pathway in the current study due to its important role in regulating angiogenesis [26]. We provided evidence that exosomes derived from hypoxia-conditioned hucMSCs strongly enhance angiogenesis via the transfer of miR-205-5p by targeting PTEN via activation of the PI3K/AKT/mTOR signalling pathway.

However, there are still several limitations associated with our work that need to be noted. First, we exclusively examined the changes in miRNA content and did not pay attention to other exosomal contents, such as lncRNAs, mRNAs, and proteins. It should not be ignored that the changes in other RNAs or proteins in hucMSC exosomes deserve further investigation. Second, miR-205-5p was chosen for study because it is the most significantly increased miRNA in hypo-Exos. Although exosomal miR-205-5p was demonstrated to play an important role in the regulation of ROMEC angiogenesis in the present study, the roles of other significantly increased miRNAs in the context of angiogenesis remain to be determined. Third, it is known that hypo-Exos can be taken up by other organs and tissues, but the side effects and the long-term impact of hypo-Exos await further investigation.

Conclusions

Taken together, our results first suggested that exosomes derived from hypoxia-conditioned hucMSCs strongly enhance endothelial cell proliferation, migration, and tube formation activities of in vitro and improve the repair functions in a preclinical rat model of premature

ovarian failure. We verified for the first time that the underlying mechanism involves hypo-Exos promoting angiogenesis via the transfer of miR-205-5p by targeting the PTEN/PI3K/AKT/mTOR signalling pathway. Our findings represent a novel strategy of applying hypo-Exos in the treatment of premature ovarian failure.

Abbreviations

norm-Exos	Normoxic-hucMSCs-exosomes
hypo-Exos	hypoxic-hucMSC-exosomes
POF	Premature ovarian failure
FSH	Follicle stimulating hormone
AMH	Decreased anti-Müllerian hormone
E2	Oestradiol
MSCs	Mesenchymal stem cells
hucMSC	Human umbilical cord
hucMSCs-exosomes	Exosomes derived from cultured hucMSCs
hypoxic-hucMSC-exosomes	Exosomes derived from hypoxic preconditioning hucMSCs
hypo-Exos	Exosomes derived from normoxic environment cultured hucMSCs
norm-Exos	Normoxic-hucMSCs-exosomes
ROMECs	Rat ovarian microvascular endothelial cells
BCA	Bicinchoninic acid
NTA	Nanoparticle tracking analysis
LSM	Laser scattering microscopy
TEM	Transmission electron microscopy
DAPI	4′,6-diamidino-2-phenylindole

Supplementary Information

The online version contains supplementary material available at https://doi.org/10.1186/s13287-024-04111-6.

Supplementary Material 1

Supplementary Material 2

Acknowledgements
Not applicable.

Author Contributions
QQ, LL, CL and YC conducted the experiment. QQ, LL, XJ, CL and LW collected the data and conducted the statistical analyses. QQ, LL, XJ, XXand LW wrote the manuscript. QQ and LL designed the research study.

Funding
This work was supported by the Natural Science Foundation of Shandong Province(No.ZR2021QH011, ZR2020QH044), and the research projects of 2022 major scientific problems and medical technology problems of China Medical Education Association(No.2022KTM024), and Shandong Medical Association Clinical Research Fund-Qilu Special Project (YXH2022ZX145). The funding body played no role in the design of the study and collection, analysis, and interpretation of data and in writing the manuscript.

Data availability
All reported data have been obtained from experiments performed in the author's laboratory. The dataset generated during the present study is available upon reasonable request from the corresponding authors.

Declarations

Ethics approval and consent to participate
The experimental procedures associated with human cells and animals were approved. (1) Title of the approved project: The effect of human umbilical cord-derived mesenchymal stem cell and its exosomes in premature ovarian failure; (2) Name of the institutional approval committee or unit: Ethics Committee of Qilu Hospital of Shandong University; (3) Approval number: KYLL-202203-013; (4) Date of approval: 18 March 2022.

Consent for publication
All authors read and approved the final manuscript.

Competing interests
The authors declare no competing interests.

Received: 10 May 2024 / Accepted: 10 December 2024
Published online: 21 December 2024

References

1. Zhou Y, Zhou J, Xu X, Du F, Nie M, Hu L, Ma Y, Liu M, Yu S, Zhang J, Chen Y. Matrigel/Umbilical Cord-Derived Mesenchymal Stem Cells Promote Granulosa Cell Proliferation and Ovarian Vascularization in a Mouse Model of Premature Ovarian Failure. Stem Cells Dev. 2021;30:782–96.
2. Bedoschi G, Navarro PA, Oktay K. Chemotherapy-induced damage to ovary: mechanisms and clinical impact. Future Oncol. 2016;12:2333–44.
3. Wang MY, Wang YX, Li-Ling J, Xie HQ. Adult Stem Cell Therapy for Premature Ovarian Failure: From Bench to Bedside. Tissue Eng Part B Rev. 2022;28:63–78.
4. Fu YX, Ji J, Shan F, Li J, Hu R. Human mesenchymal stem cell treatment of premature ovarian failure: new challenges and opportunities. Stem Cell Res Ther. 2021;12:161.
5. He Y, Chen D, Yang L, Hou Q, Ma H, Xu X. The therapeutic potential of bone marrow mesenchymal stem cells in premature ovarian failure. Stem Cell Res Ther. 2018;9:263.
6. Prockop DJ, Brenner M, Fibbe WE, Horwitz E, Blanc KL, Phinney DG, Simmons PJ, Sensebe L, Keating A. Defining the risks of mesenchymal stromal cell therapy. Cytotherapy. 2010;12:576–8.
7. Nikfarjam S, Rezaie J, Zolbanin NM, Jafari R. Mesenchymal stem cell derived-exosomes: a modern approach in translational medicine. J Transl Med. 2020;18:449.
8. Ma ZJ, Yang JJ, Lu YB, Liu ZY, Wang XX. Mesenchymal stem cell-derived exosomes: Toward cell-free therapeutic strategies in regenerative medicine. World J Stem Cells. 2020;12:814–40.
9. Qu Q, Liu L, Cui Y, Liu H, Yi J, Bing W, Liu C, Jiang D, Bi Y. miR-126-3p containing exosomes derived from human umbilical cord mesenchymal stem cells promote angiogenesis and attenuate ovarian granulosa cell apoptosis in a preclinical rat model of premature ovarian failure. Stem Cell Res Ther. 2022;13:352.
10. Krock BL, Skuli N, Simon MC. Hypoxia-induced angiogenesis: good and evil. Genes Cancer. 2011;2:1117–33.
11. Yang Y, Lee EH, Yang Z. Hypoxia-Conditioned Mesenchymal Stem Cells in Tissue Regeneration Application. Tissue Eng Part B Rev. 2022;28:966–77.
12. Robinson RS, Woad KJ, Hammond AJ, Laird M, Hunter MG, GE Mann. Angiogenesis and vascular function in the ovary. Reproduction. 2009;138:869–81.
13. Tamanini C, De Ambrogi M. Angiogenesis in developing follicle and corpus luteum. Reprod Domest Anim. 2004;39:206–16.
14. Qu Q, Pang Y, Zhang C, Liu L, Bi Y. Exosomes derived from human umbilical cord mesenchymal stem cells inhibit vein graft intimal hyperplasia and accelerate reendothelialization by enhancing endothelial function. Stem Cell Res Ther. 2020;11:133.
15. Qu Q, Wang L, Bing W, Bi Y, Zhang C, Jing X, Liu L. miRNA-126-3p carried by human umbilical cord mesenchymal stem cell enhances endothelial function through exosome-mediated mechanisms in vitro and attenuates vein graft neointimal formation in vivo. Stem Cell Res Ther. 2020;11:464.
16. Sakurai T, Suzuki K, Yoshie M, Hashimoto K, Tachikawa E, Tamura K. Stimulation of tube formation mediated through the prostaglandin EP2 receptor in rat luteal endothelial cells. J Endocrinol. 2011;209:33–43.
17. Pusztaszeri MP, Seelentag W, Bosman FT. Immunohistochemical expression of endothelial markers CD31, CD34, von Willebrand factor, and Fli-1 in normal human tissues. J Histochem Cytochemistry. 2006;54:385–95.
18. Bing W, Pang X, Qu Q, Bai X, Yang W, Bi Y, Bi X. Simvastatin improves the homing of BMSCs via the PI3K/AKT/miR-9 pathway. J Cell Mol Med. 2016;20:949–61.
19. Zhuang Y, Cheng M, Li M, Cui J, Huang J, Zhang C, Si J, Lin K, Yu H. Small extracellular vesicles derived from hypoxic mesenchymal stem cells promote vascularized bone regeneration through the miR-210-3p/EFNA3/PI3K pathway. Acta Biomater. 2022;150:413–26.

20. Kalluri R, LeBleu VS. The biology, function,biomedical applications of exosomes. Science. 2020;367:6977.
21. Thery C, Zitvogel L, Amigorena S. Exosomes: composition, biogenesis and function. Nat Rev Immunol. 2002;2:569–79.
22. Mathieu M, Martin-Jaular L, Lavieu G, Thery C. Specificities of secretion and uptake of exosomes and other extracellular vesicles for cell-to-cell communication. Nat Cell Biol. 2019;21:9–17.
23. Chen S, Sun F, Qian H, Xu W, Jiang J. (2022). Preconditioning and Engineering Strategies for Improving the Efficacy of Mesenchymal Stem Cell-Derived Exosomes in Cell-Free Therapy. Stem Cells Int 2022:1779346.
24. Wen S, Stolarov J, Myers MP, Su JD, Wigler MH, Tonks NK, DL Durden. PTEN controls tumor-induced angiogenesis. Proc Natl Acad Sci U S A. 2001;98:4622–7.
25. Hamada K, Sasaki T, Koni PA, Natsui M, Kishimoto H, Sasaki J, Yajima N, Horie Y, Hasegawa G, Naito M, Miyazaki J, Suda T, Itoh H, Nakao K, Mak TW, Nakano T, Suzuki A. The PTEN/PI3K pathway governs normal vascular development and tumor angiogenesis. Genes Dev. 2005;19:2054–65.
26. Karar J, Maity A. PI3K/AKT/mTOR Pathway in Angiogenesis. Front Mol Neurosci. 2011;4:51.
27. Jiang BH, Liu LZ. PI3K/PTEN signaling in angiogenesis and tumorigenesis. Adv Cancer Res. 2009;102:19–65.
28. Morgan S, Anderson RA, Gourley C, Wallace WH, Spears N. How do chemotherapeutic agents damage the ovary? Hum Reprod Update. 2012;18:525–35.
29. Oltra M, Vidal-Gil L, Maisto R, J Sancho-Pelluz and, Barcia JM. Oxidative stress-induced angiogenesis is mediated by miR-205-5p. J Cell Mol Med. 2020;24:1428–36.
30. Nguyen LT, Tran NT, Than UTT, Nguyen MQ, Tran AM, Do PTX, Chu TT, Nguyen TD, Bui AV, Ngo TA, Hoang VT, NTM Hoang. Optimization of human umbilical cord blood-derived mesenchymal stem cell isolation and culture methods in serum- and xeno-free conditions. Stem Cell Res Ther. 2022;13:15.
31. Estrada JC, Albo C, Benguria A, Dopazo A, Lopez-Romero P, Carrera-Quintanar L, Roche E, Clemente EP, Enriquez JA, Bernad A, Samper E. Culture of human mesenchymal stem cells at low oxygen tension improves growth and genetic stability by activating glycolysis. Cell Death Differ. 2012;19:743–55.
32. Das R, Jahr H, van Osch GJ, Farrell E. The role of hypoxia in bone marrow-derived mesenchymal stem cells: considerations for regenerative medicine approaches. Tissue Eng Part B Rev. 2010;16:159–68.
33. Wang X, Tang Y, Liu Z, Yin Y, Li Q, Liu G, Yan B. (2021). The Application Potential and Advance of Mesenchymal Stem Cell-Derived Exosomes in Myocardial Infarction. Stem Cells Int 2021:5579904.
34. Mu J, Li L, Wu J, Huang T, Zhang Y, Cao J, Ma T, Chen J, Zhang C, Zhang X, Lu T, Kong X, Sun J, Gao J. Hypoxia-stimulated mesenchymal stem cell-derived exosomes loaded by adhesive hydrogel for effective angiogenic treatment of spinal cord injury. Biomater Sci. 2022;10:1803–11.
35. Wang J, Wu H, Peng Y, Zhao Y, Qin Y, Zhang Y, Xiao Z. Hypoxia adipose stem cell-derived exosomes promote high-quality healing of diabetic wound involves activation of PI3K/Akt pathways. J Nanobiotechnol. 2021;19:202.

Publisher's note